

## **Computational Simulation of Mechanical Behavior of Semi-Crystalline Polymers with Randomly Distributed Rubber Particles**

M. Uchida<sup>1</sup>, N. Tada<sup>1</sup> and Y. Tomita<sup>2</sup>

### **Summary**

Micro- to mesoscopic deformation behavior of semi-crystalline polymer with randomly distributed rubber particles is evaluated by numerical simulation. In this model, dimension of mesostructure is identified by volume fraction of interface region around the rubber particles. The effects of strain rate and size of mesostructure on macroscopic stress-strain relation and strain distribution in mesoscopic area are discussed. In the earlier stage of deformation, the slope of stress-strain relation changes by rubber particle size while stress in the following deformation is mainly affected by the tensile strain rate. The anisotropic deformation in lamellar oriented interface region causes change in the strain distribution depending on size of mesostructure.

### **Introduction**

In order to improve the toughness of polymeric materials, rubber particles are often blended into the polymer matrix, which leads to lower stress triaxiality in the polymer matrix. In the case of semi-crystalline polymer matrix, mesostructures become very complex by the introduction of rubber particle, and they affect the macroscopic mechanical behaviors. For example, a ligament thickness between rubber particles is known as a key parameter to evaluate toughness of rubber blended semi-crystalline polymers[1]. This is closely related to the preferential orientation of lamellae around the rubber particle [2, 3].

Relationship between mechanical behavior of rubber blended glassy polymer and its material morphology such as volume fraction, distribution of rubber particles or heterogeneity of glassy polymer matrix is clarified by the numerical investigation [4-6]. Several papers concerning the modeling of mechanical deformation behavior of rubber blended semi-crystalline polymers have also been published [7, 8]. However, the constitutive relation of semi-crystalline polymer matrix is modeled by the macroscopic hardening theory.

The authors proposed a multi-scale model of rubber blended semi-crystalline polymer by using large deformation finite element homogenization method [9]. This model can evaluate the mechanical behavior and evolution of material morphology in the micro- to mesoscopic scales of material. In this paper, the effect of tensile strain rate and size of rubber particle is investigated by computational simu-

---

<sup>1</sup>Graduate School of Natural Science and Technology, Okayama University, Japan

<sup>2</sup>Graduate School of Engineering, Kobe University, Japan

lation of tensile deformation of High Density Polyethylene (HDPE) with randomly distributed rubber particles.

### Constitutive Equation

In this study, mesostructure of rubber blended semi-crystalline polymer is divided into the three phases; rubber particle, lamellar oriented interface region and isotropic matrix. Rubber particles are replaced by voids on the assumption that material contains cavitated rubber particles[4]. Mechanical behavior in lamellar oriented interface region and isotropic matrix is described as follows.

The mechanical behavior of the lamellar oriented interface region is based on the deformation of crystalline and amorphous phases which consist of microscopic area of semi-crystalline polymers. The crystalline plasticity theory with the penalty method[10] and the nonaffine molecular chain network theory[11] were employed to describe deformation behaviors of each phases.

The constitutive equation for the crystalline phase is expressed as[10]

$$\overset{\nabla}{S}_{ij} = (D_{ijkl}^C - \lambda_0 c_i c_j c_k c_l) d_{kl} - \sum_{(\alpha)} R_{ij}^{(\alpha)} \dot{\gamma}_{pC}^{(\alpha)}, \quad (1)$$

$$R_{ij}^{(\alpha)} = D_{ijkl}^C P_{kl}^{(\alpha)} + (W_{ik}^{(\alpha)} \sigma_{kj} + \sigma_{ik} W_{kj}^{(\alpha)}) \dot{\gamma}_{pC}^{(\alpha)}, \quad W_{ij}^{(\alpha)} = \frac{1}{2} (s_i^{(\alpha)} m_j^{(\alpha)} - m_i^{(\alpha)} s_j^{(\alpha)}),$$

where  $\overset{\nabla}{S}$  is the Jaumann rate of Kirchhoff stress,  $D_{ijkl}^C$  is anisotropic elastic modulus tensor,  $d_{ij}$  is the total strain rate tensor,  $c_i$  is the unit vector of chain direction,  $\dot{\gamma}_{pC}^{(\alpha)}$  is shear strain rate on the  $\alpha$ th slip system,  $P_{ij}^{(\alpha)} = (s_i^{(\alpha)} m_j^{(\alpha)} + m_i^{(\alpha)} s_j^{(\alpha)}) / 2$  is the Schmid tensor and  $\lambda_0$  is the penalty constant which represents the chain directional stiffness.

The constitutive equation for the amorphous phase is expressed as[11]

$$\overset{\nabla}{S}_{ij} = D_{ijkl}^A d_{kl} - \dot{\gamma}_{pA} \frac{2G}{\sqrt{2}\tau^*} (\sigma'_{ij} - B_{ij}), \quad (2)$$

where  $D_{ijkl}^A$  is isotropic elastic modulus tensor,  $\dot{\gamma}_{pA}$  is plastic shear strain rate,  $\tau^*$  is the applied shear stress.  $B_{ij}$  in Eq. (2) is the back-stress tensor and the principal components are expressed by employing the eight-chain model[12],

$$B_i = \frac{1}{3} C^R \sqrt{N} \frac{V_i^2 - \lambda^2}{\lambda} L^{-1} \left( \frac{\lambda}{\sqrt{N}} \right), \quad (3)$$

where  $\lambda^2 = (V_1^2 + V_2^2 + V_3^2) / 3$ ,  $V_i$  is the principal plastic stretch,  $N$  is the average number of segments in a single chain,  $C^R$  is a rubber elastic modulus, and

$L(x) = \coth(x) - 1/x$  is the Langevin function. In the nonaffine model,  $N$  may change depending on the distortion  $\xi$ [11]. The simplest expression of the number of entangled points is  $N = N_0 \exp\{c(1 - \xi)\}$  with  $\xi = 1$  in the reference state, and  $N_0$  is the number of segments in a single chain in the reference state and  $c$  is a material constant.

On the other hand, constitutive equation for isotropic matrix is expressed as following macroscopic elasto-visco-plastic constitutive equation[8],

$$\sigma_{eq} = \sigma_0 \left[ h \varepsilon_{eq} + q^{m^M} \left\{ 1 + \left( \frac{\dot{\varepsilon}_{eq}}{q \dot{\gamma}_0^M} \right)^2 \right\}^{m^M/2} \right], \quad (4)$$

where  $\sigma_0$ ,  $\dot{\gamma}_0^M$ ,  $h$  and  $q$  are material constants,  $m^M$  is strain rate sensitivity exponent,  $\sigma_{eq} = 3\sigma'_{ij}\sigma'_{ij}/2$  and  $\dot{\varepsilon}_{eq} = 2\dot{\varepsilon}_{ij}\dot{\varepsilon}_{ij}/3$  are equivalent stress and strain rate,  $\varepsilon_{eq} = \int_0^t \dot{\varepsilon}_{eq} dt$  is equivalent strain.

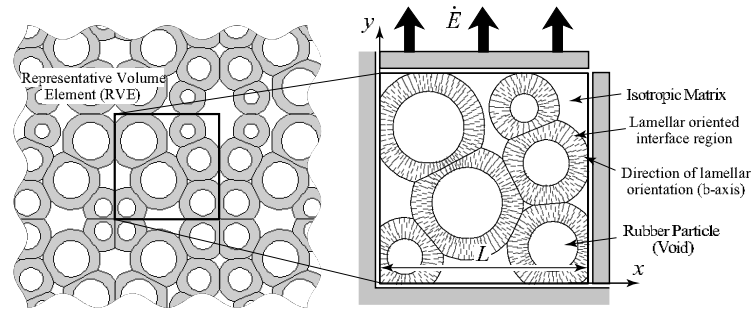
### Computational Model

Figure 1 shows computational model of mesostructures of semi-crystalline polymer with randomly distributed rubber particles. As mentioned above, mesostructures of rubber blended semi-crystalline polymer is divided into three region; rubber particle, lamellar oriented interface region and isotropic matrix. The thickness of interface region is approximately  $0.3 \mu\text{m}$  for HDPE[3]. Therefore, dimension of mesostructure is identified by volume fraction of interface region in this model. Fig. 1(a) shows Representative Volume Element (RVE) model of mesostructure of material and boundary conditions for RVE, (b) shows finite element mesh divisions for  $L=1.0\mu\text{m}$ ,  $L=2.0\mu\text{m}$  and  $L=3.0\mu\text{m}$ . Here, location and volume fraction of rubber particles (voids) are fixed. In the interface region, b-axis of crystalline lamella is oriented to the normal direction to the rubber particle/semi-crystalline polymer interface as shown in Fig. 1(a), which causes anisotropic deformation in interface region.

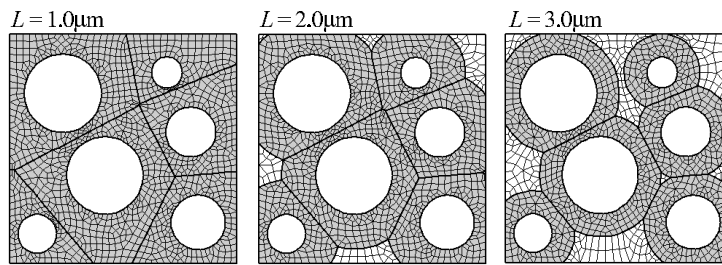
In this paper, the effect of mesostructure size  $L$  and macroscopic tensile strain rate  $\dot{E}$  on deformation behavior of rubber blended semi-crystalline polymer is investigated. Table 1 shows simulation conditions. For three different sizes of mesostructure shown in Fig. 1(b), tensile deformation of three different strain rate,  $\dot{E} = 1.0 \times 10^{-3}$ ,  $\dot{E} = 1.0 \times 10^{-2}$  and  $\dot{E} = 1.0 \times 10^{-1}$  are applied, respectively. The material parameters for HDPE are described in refs.[8, 11].

### Result and Discussion

Figure 2 shows relationships between macroscopic true stress and strain for all conditions in Table 1. Macroscopic stress strain relation of rubber blended semi-crystalline polymer shows no clear yielding behavior which is attributable to the continuous local yielding in the mesoscopic area caused by the heterogeneity of



(a) RVE Model of mesostructure of rubber blended semi-crystalline polymer.



(b) Mesh divisions for each model size.

Figure 1: Computational model

mesoscopic morphology. Macroscopic response depends on not only tensile strain rate but also rubber particle size. In the earlier stage of deformation, the slope of stress-strain relation changes by rubber particle size while stress in the following deformation is mainly affected by macroscopic tensile strain rate. With the decrease in size of rubber particles, local yielding is promoted by heterogeneity of lamellar oriented interface region. This leads to lower stress in the earlier stage of deformation for smaller sized rubber particles blended polymers.

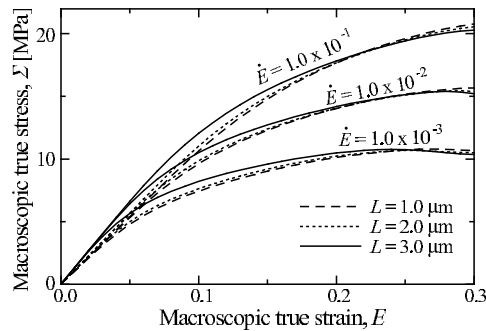


Figure 2: Macroscopic true stress vs. strain

Figure 3 shows equivalent strain distributions at different degree of deforma-

Table 1: Simulation conditions

Condition	Length of RVE, $L$ [ $\mu\text{m}$ ]	Macroscopic tensile strain rate, $\dot{E}$
1	1.0	$1 \times 10^{-3}$
2		$1 \times 10^{-2}$
3		$1 \times 10^{-1}$
4	2.0	$1 \times 10^{-3}$
5		$1 \times 10^{-2}$
6		$1 \times 10^{-1}$
7	3.0	$1 \times 10^{-3}$
8		$1 \times 10^{-2}$
9		$1 \times 10^{-1}$

tion for macroscopic tensile strain rates  $\dot{E} =$  (a)  $1.0 \times 10^{-3}$  and (b)  $1.0 \times 10^{-1}$ . In Figs.3 (a) and (b), upper and lower figures show  $L=0.10\mu\text{m}$  and  $L=0.30\mu\text{m}$ , respectively. With the increase of macroscopic strain, locally strained zones appear in the mesostructure, and degree of equivalent strain in the interface region is larger than that of isotropic matrix.

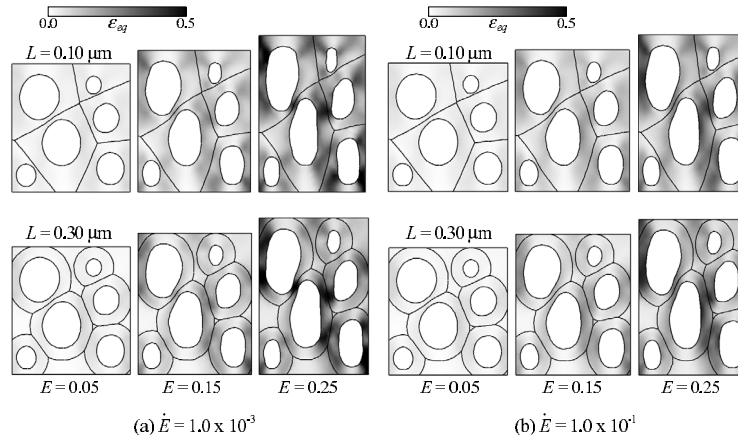


Figure 3: Equivalent strain distribution

Comparison between the results for  $L=0.10\mu\text{m}$  and  $L=0.30\mu\text{m}$  shows the slight difference of equivalent strain distribution. In the case of  $L=0.10\mu\text{m}$ , locally strained zone appears along  $\pm 45$  directions to connect rubber particles. On the other hand, equivalent strain in the case of  $L=0.30\mu\text{m}$  tends to concentrate at the ligament region normal to the tensile load. This tendency is seen in both of  $\dot{E} = 1.0 \times 10^{-3}$  and  $1.0 \times 10^{-1}$ . This result is caused by the anisotropic deformation behavior of lamellar oriented interface region. Shearing deformation in amorphous phase and slip deformation in crystalline phase are easy to cause along  $\pm 45$  directions in interface region. As a result, localized deformations along those directions are markedly in-

tensified with the increase in volume fraction of lamellar oriented interface region, namely decrease in ligament thickness between rubber particles.

### References

1. Wu, S. (1985): "Phase structure and adhesion in polymer blends, A criterion for rubber toughening", *Polymer*, Vol. 26, pp.1855-1863.
2. Muratoglu, O. K., Argon, A. S. and Cohen, R. E. (1995): "Crystalline morphology of polyamide-6 near planar surfaces", *Polymer*, Vol.36, pp.2143-2152.
3. Bartczak, Z., Argon, A. S., Cohen, R. E. and Weinberg, M. (1999): "Toughness mechanism in semi- crystalline polymer blends: I. High-density polyethylene toughened with rubbers", *Polymer*, Vol.40, pp.2331-2346.
4. Steenbrink, A. C. and Van der Giessen, E. (1998): "Strain localization and void growth in polymers", *Material Instabilities in Solids, Edited by Borst, R. and Van der Giessen, E.*, pp.287-302, John Wiley & Sons Ltd.
5. Tomita, Y. and Lu, W. (2002): "Characterization of micro- to macroscopic response of polymers containing second- phase particles under macroscopically uniform deformation", *International Journal of Solids and Structures*, Vol.39, pp.3409-3428.
6. Tomita, Y. and Uchida, M. (2004): "Computational evaluation of micro- to macroscopic deformation behavior of amorphous polymer with slightly heterogeneous distribution of initial shear strength", *IUTAM Symposium on Meso-scopic Dynamics in Fracture Process and Strength of Materials*, pp.245-254, Kluwer.
7. Tzika, P. A., Boyce, M. C. and Parks, D. M. (2000): "Micromechanics of Deformation in Particle-Toughened Polyamides", *Journal of the Mechanics and Physics of Solids*, Vol.48, pp.1893-1929.
8. Van Dommelen, J. A. W., Brekelmans, W. A. M. and Baaijens, F. P. T. (2003), "Micromechanical modeling of particle- toughening of polymers by locally induced anisotropy", *Mechanics of Materials*, Vol.35, pp.845- 863.
9. Uchida, M., Tada, N. and Tomita, Y. (2006): "Multiscale Modeling of Deformation Behavior of Rubber Blended Semi-Crystalline Polymer", *Transactions of the Japan Society of Mechanical Engineers*, Vol. 73, pp.73-79 (in Japanese).
10. Uchida, M. and Tomita, Y. (2002): "Deformation of Crystalline Polymers Containing Amorphous Phase", *Proceedings of CMD2002*, pp.111-112 (in Japanese).

11. Tomita, Y., Adachi, T. and Tanaka, S. (1997): “Modelling and Application of Constitutive Equation for Glassy Polymer Based on Nonaffine Network Theory”, *European Journal of Mechanics - A/Solids*, Vol.16, pp.745-755.
12. Arruda, E. M. and Boyce, M. C. (1993); “A Three-dimensional constitutive model for the large stretch behavior of rubber elastic materials”, *Journal of the Mechanics and Physics of Solids*, Vol.41, pp.389-412.

